JACS
JOURNAL OF THE AMERICAN CHEMICAL SOCIETY
Communication
pubs.acs.org/JACS

Genetic Encoding of Photocaged Cysteine Allows Photoactivation of TEV Protease in Live Mammalian Cells

Duy P. Nguyen, Mohan Mahesh, Simon J. Elsässer, Susan M. Hancock, Chayasith Uttamapinant, and Jason W. Chin*

Medical Research Council Laboratory of Molecular Biology, Francis Crick Avenue, Cambridge CB2 0QH, United Kingdom

Supporting Information

ABSTRACT: We demonstrate the evolution of the PylRS/tRNA$_{CUA}$ pair for genetically encoding photocaged cysteine. By characterizing the incorporation in *Escherichia coli* and mammalian cells, and the photodeprotection process *in vitro* and in mammalian cells, we establish conditions for rapid efficient photodeprotection to reveal native proteins in live cells. We demonstrate the utility of this approach by rapidly activating TEV protease following illumination of single cells.

Insight into dynamic processes in cells and organisms would be facilitated by approaches to control protein function with spatial and temporal precision. Rapid control of protein function with light provides a promising route to perturb processes more rapidly than most biological adaptations, providing information that cannot be obtained by gene knockouts or knockdowns. Several exciting strategies have emerged for the photocontrol of protein function, including the control of protein localization or assembly mediated by the genetic fusion of photoresponsive interaction domains to target proteins (or their fragments), and the introduction of photocaged amino acids in place of a key residue within a protein.[1−7]

Strategies that photocage key residues within a target protein have several advantages: (i) structural information and bioinformatics can be used to reliably choose positions (e.g., key catalytic residues, residues at a protein interface, or residues targeted for post-translational modifications) where the introduction of a photocage will allow photocontrol; and (ii) following illumination, the structure, function, activity and localization of the resulting protein are entirely native.

Proteins bearing photocaged amino acids have been synthesized by chemical ligation and introduced into cells via microinjection, and more recently synthesized directly in cells via genetic code expansion. Photocaged lysine, tyrosine, and serine have been site specifically incorporated in place of key residues, allowing photocontrol of nuclear localization sequences, kinases, and other enzymes, and photocontrol of the sites of post-translational modification.[2,4,8−11] These approaches have revealed the kinetics, and feedback/feedforward contributions in elementary steps of complex signaling pathways with high spatial and temporal resolution.[1,4,8]

Key cysteine residues are found in many classes of proteins including: phosphatases, ubiquitin ligases, cysteine proteases (including caspases and deubiquitinases) and inteins. Cysteine residues are also the sites of protein palmitoylation and form disulfide bonds in proteins. The ability to (i) genetically encode the site-specific incorporation of a photocaged cysteine residue into a target protein and (ii) rapidly and cleanly convert the caged cysteine to cysteine upon illumination of living cells would provide an important approach for controlling diverse biological processes.

The incorporation of an *ortho*-nitrobenzyl (ONB) caged cysteine **1** has been reported in yeast using the *Escherichia coli* (*E. coli*) leucyl-tRNA synthetase/tRNA$_{CUA}$ pair.[11] However, **1** has not been incorporated in other host organisms. Moreover 70% deprotection of this amino acid in yeast lysate required 20 min illumination with a hand-held UV lamp of unknown spectral distribution and power, and photodecaging of this amino acid has not been extended to living cells.

The pyrrolysyl-tRNA synthetase (PylRS)/tRNA$_{CUA}$ pair from methanogenic archaeal species, including *Methanosarcina barkeri* (*Mb*), *Methanosarcina mazei* (*Mm*) and their synthetically evolved variants, have been used to direct the site-specific incorporation of unnatural amino acids[12] into proteins produced in *E. coli*, yeast, mammalian cells, *Caenorhabditis elegans*, *Drosophila melanogaster*, and *Arabidopsis thaliana*.[13−18] Here we demonstrate the evolution of the PylRS/tRNA$_{CUA}$ pair for genetically encoding photocaged cysteine. By carefully characterizing the incorporation in *E. coli* and mammalian cells, and the photodeprotection process *in vitro* and in mammalian cells, we establish conditions for rapid near-quantitative photodeprotection to reveal native proteins in live cells. We demonstrate the utility of this approach by rapidly activating TEV protease following illumination of single cells.

We initially evolved a synthetase/tRNA$_{CUA}$ pair for **1** (Figure 1a). To evolve the orthogonal *Mb*PylRS/tRNA$_{CUA}$ pair for the site-specific incorporation of **1**, we created a library of *Mb*PylRS mutants in which five residues in the amino acid binding site (N311, C313, V366, W382, and G386) were randomized to all possible natural amino acids. We performed three rounds of alternating positive and negative selection on the library in *E. coli*, as previously described.[17] Eighty out of the 96 selected synthetase/tRNA$_{CUA}$ pairs we screened from the selection conferred survival on *E. coli* (bearing a chloramphenicol acetyl transferase gene with an amber codon at position 112) on 350 μg/mL chloramphenicol in the presence of **1** but did not confer survival on 50 μg/mL chloramphenicol in the absence of **1**. This suggests that the majority of the selected synthetases are

Received: November 29, 2013
Published: January 30, 2014

   dx.doi.org/10.1021/ja412191m | J. Am. Chem. Soc. 2014, 136, 2240−2243

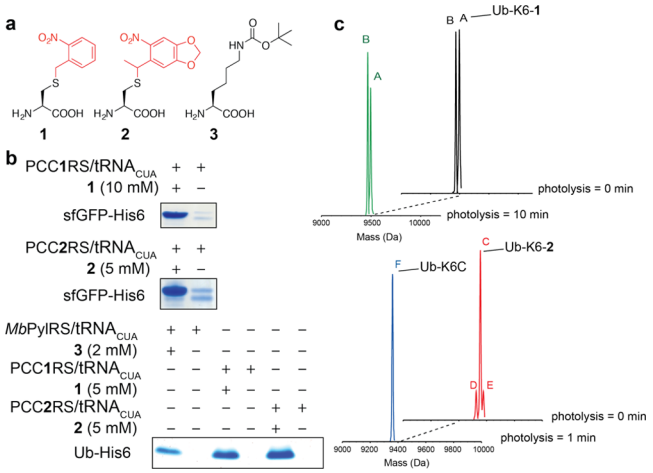

Figure 1. Genetic incorporation of photocaged cysteines in *Escherichia coli* (*E. coli*). (a) Chemical structures of **1**, **2**, and **3**. (b) sfGFP and ubiquitin incorporating **1** or **2**, overexpressed in *E. coli* and Ni-NTA purified. (c) ESI-MS demonstrates the incorporation of **1** into ubiquitin in *E. coli* (A) observed: 9496.7 Da, expected: 9497.6 Da). A second peak (B) is consistent with nitro reduction of **1** to the corresponding amine. ESI-MS analyses revealed no decaging of **1** after 10 min of illumination at 365 nm (~35 mW/cm^2). In contrast, **2** is minimally reduced (peak C; observed: 9554.8 Da, expected: 9553.6 Da), and conversion of Ub-K6-**2** to Ub-K6C (peak F; observed: 9361.3 Da, expected: 9362.6 Da) after 1 min of illumination is quantitative. (D) corresponds to a reduced species and (E) to a salt adduct (see Supporting Information [SI], Figure S1a–d, for additional spectra and analyses).

specific for the unnatural amino acid. The majority of the selected clones had the mutations: N311M, C313Q, V366G, W382N, and one nonprogrammed mutation, R85H. We named this synthetase PCC**1**RS (SI, Table S1). Production of full-length sfGFP from *E. coli* bearing *sfGFP-N150TAG* (A gene for superfolder GFP with an amber codon at position 150) and the PCC**1**RS/tRNA$_{CUA}$ pair was dependent on the addition of **1** (Figure 1b). Similarly, production of ubiquitin (Ub) from *E. coli* bearing *UbK6TAG* and the PCC**1**RS/tRNA$_{CUA}$ pair was dependent on the addition of **1** (Figure 1b). SfGFP-N150-**1** and Ub-K6-**1** were produced in good yield (~5 mg/L of culture). Electrospray ionization mass spectrometry (ESI-MS) confirmed the genetically directed incorporation of **1** in recombinant proteins (Figure 1c and SI, Figure S1a), but also demonstrated that a substantial portion of the protein contained a mass consistent with reduction of the nitro group within the compound to an amine.

Following irradiation of Ub-K6-**1** with 365 nm (~35 mW/cm^2) light for 10 min, the ONB caging group on ubiquitin remained intact (Figure 1c and SI Figure S1c). While it is possible to remove this group with shorter wavelengths, longer illumination or more powerful illumination, we investigated the genetic encoding of a new photocaged cysteine.

We designed and synthesized a photocaged cysteine **2** that should be efficiently uncaged with nonphototoxic light at 365 nm (Figure 1a; see SI for synthesis). The caging group in **2** can be efficiently removed by illumination at 365 nm (as a result of the bathochromic shift in the absorbance spectrum of the caging group).[19] The application of non-phototoxic light to decage **2** minimizes potential photoreactions of nucleic acids, destruction of disulfides, and other cellular damage. Moreover, photolysis of **2** generates a ketone byproduct that will not undergo undesired reactions with proteins.

To evolve a synthetase for the incorporation of **2**, we repeated the selection with **2**, using the library used to select the synthetase variant specific for **1**. Out of 96 clones from the final round of positive selection, screened as described above, one conferred survival on 350 μg/mL chloramphenicol in the presence of **2** but did not survive at 50 μg/mL chloramphenicol in the absence of unnatural amino acid. The selected synthetase contained three mutations in the active site: N311Q, C313A and V366M, with respect to *Mb*PylRS, and was named PCC**2**RS. Expression of ubiquitin and sfGFP genes containing an amber codon in the presence of PCC**2**RS/tRNA$_{CUA}$ pair was efficient (~4 mg/L of culture) and dependent on the presence of **2** (Figure 1b). ESI-MS confirmed the incorporation of **2** in ubiquitin and sfGFP (Figure 1c). Ubiquitin containing **2** is quantitively decaged upon irradiation at 365 nm (~35 mW/cm^2) for 1 min (Figure 1c and SI, Figure S1d). Therefore, **2**, unlike **1**, is incorporated with minimal reduction in *E. coli*, and is quantitatively decaged. On the basis of these advances we proceeded to investigate the genetic incorporation of **2** into proteins in mammalian cells.

To demonstrate the genetically directed site-specific incorporation of **2** into a protein in mammalian cells, we introduced the *Mm*PCC**2**RS (a variant of *Mm*PylRS containing the mutations discovered in *Mb*PylRS that direct the incorporation of **2**)/tRNA$_{CUA}$ pair into a human embryonic kidney 293T (HEK293T) cell line stably expressing *mCherry-TAG-eGFP-HA* gene (a fusion between the genes encoding a red fluorescent (mCherry) protein and a green fluorescent protein (eGFP) and the human influenza hemagglutinin (HA) tag separated by the amber codon (TAG)). Anti-HA immunobloting and fluorescence microscopy confirmed that the expression of full-length mCherry-eGFP-HA is dependent upon the addition of **2** (Figure 2**a** and SI, Figure S2a). The incorporation efficiency of **2** is comparable to that of N$^{\varepsilon}$-*tert*-butyloxycarbonyl-L-lysine **3**, a good substrate for the PylRS/tRNA$_{CUA}$ pair[18,20] (Figure 2a). To demonstrate the generality of this approach for incorporating **2** into proteins we expressed an *sfGFP-N150TAG* gene in HEK293T cells in the presence of the *Mm*PCC**2**RS/tRNA$_{CUA}$ pair and **2** and purified the protein (Figure 2b). ESI-MS demonstrated the genetically directed incorporation of **2** into sfGFP (sfGFP-N150-**2** (Figure 2b and SI Figure S2b) in mammalian cells without reduction. Illumination of HEK293T cells expressing sfGFP-**2** (1 min, 365 nm, ~4 mW/cm^2), followed by purification of sfGFP and ESI-MS demonstrates the efficient conversion of **2** to cysteine in the protein (90% deprotection with 1/10th of the power used for quantitative deprotection *in vitro*). This demonstrates that genetically encoded **2** can be cleanly and efficiently decaged in proteins expressed in live mammalian cells (Figure 2c and SI, Figure S2b,c).

To exemplify the photocontrol of protein function in mammalian cells via the genetically directed incorporation of **2** we replaced the catalytic cysteine (C151) in Tobacco Etch Virus (TEV) protease. We synthesized TEV protease incorporating **2** (TEV-C151-**2**) in HEK293T cells, bearing TEV-C151-TAG and the *Mm*PCC**2**RS/tRNA$_{CUA}$ pair (Figure 3a,b).

To report on TEV protease activity in cells we used an ECFP-TevS-YFP-V5 fusion protein containing a TEV cleavage site (TevS) at the linker between ECFP (enhanced cyan fluorescent protein), YFP (yellow fluorescent protein), and C-

dx.doi.org/10.1021/ja412191m | *J. Am. Chem. Soc.* 2014, 136, 2240–2243

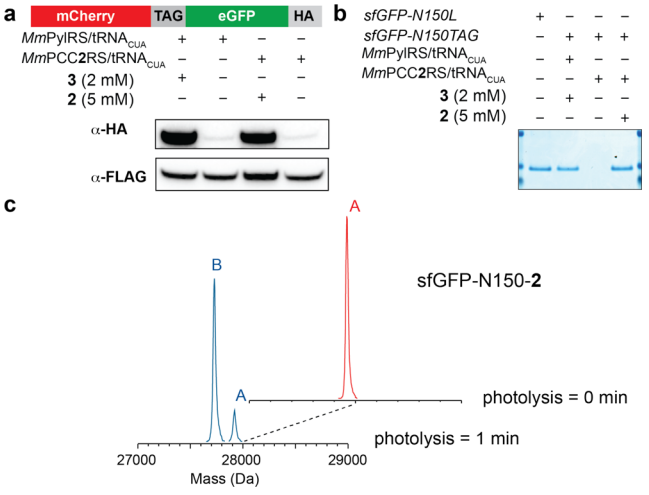

Figure 2. Genetically directed incorporation and photodecaging of **2** in mammalian cells. (a) Immunoblotting of proteins from HEK293T cells expressing *mCherry-TAG-egfp-ha* transfected with *Mm*PCC**2**RS-FLAG/tRNA$_{CUA}$ pair in the presence or absence of **2** (5 mM). (b) SDS-PAGE analysis confirmed the expression of sfGFP-N150-**2** in HEK293T cells in the presence of the *Mm*PCC**2**RS/tRNA$_{CUA}$ pair and **2**. The full-length sfGFP was purified by immunoprecipitation using an anti-GFP antibody. (c) Efficient conversion of SfGFP-N150-**2** (A; observed: 27921 Da, expected: 27922 Da) expressed and illuminated in live HEK293T cells to SfGFP−N150-C (B; observed: 27729 Da, expected: 27728 Da) (See SI Figure S2b,c, for detailed analyses).

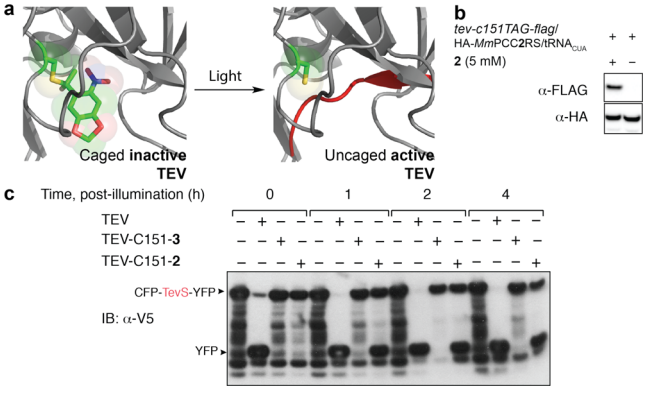

Figure 3. Photocontrol of TEV protease activity in mammalian cells. (a) Strategy for photoactivating TEV protease. Caging a catalytic cysteine (C151) in TEV protease deactivates it. TEV protease can be rapidly activated by removing the caging group with light. (b) Site-specific incorporation of **2** in TEV protease. Full-length TEV-C151-**2** was expressed in HEK293T cells in the presence of **2** and the *Mm*PCC**2**RS/tRNA$_{CUA}$ pair. (c) TEV protease can be efficiently activated with light in HEK293T cells. Cells were illuminated (1 min, 365 nm,~4 mW/cm^2). All cells contained the reporter of TEV protease activity.

terminal V5 tag.[21] This TEV protease sensor allows activity to be monitored by both western blot and Förster resonance energy transfer (FRET).

Control HEK293T cells expressing only the protease sensor produced full-length fusion protein and a series of smaller V5 immunoreactive species that may result from nonspecific proteolysis of the ECFP portion of the reporter (Figure 3c, lanes 1, 5, 9 and 13). The addition of the wild-type TEV protease causes cleavage of the TEV site in both the full-length sensor and the smaller V5 immunoreactive species, resulting in the appearance of a single YFP-V5 immuno-responsive cleavage product (Figure 3c: lanes 2, 6, 10, 14, and SI, Figure S3). No cleavage of the sensor was observed when **2** or **3** was incorporated into TEV protease in place of the catalytic cysteine, demonstrating that this is sufficient to abrogate TEV protease activity (Figure 3c: lanes 3 and 4). Upon illumination (1 min, 365 nm, 4 mW/cm^2) of cells bearing TEV-C151-**2**, we observe an increase in the YFP-V5 cleavage product resulting from photoactivation of TEV-C151-**2** to TEV protease (Figure 3c: lanes 4, 8, 12, 16). Illumination of control cells expressing TEV-C151-**3** did not result in cleavage of the reporter, confirming the specificity of the approach (Figure 3c: lanes 3, 7, 11, 15). In these experiments the extent of reporter cleavage following photoactivation is less than with wild-type TEV protease, and this is in part because the experiment is a three-plasmid transient transfection, and not all cells contain the reporter, synthetase, tRNA, and TEV protease genes.

We subsequently monitored TEV protease activity over 4 h by FRET fluorescence-activated cell sorting (FRET-FACS) (Figure 4 and SI, Figure S4a−f). Control FRET-FACS

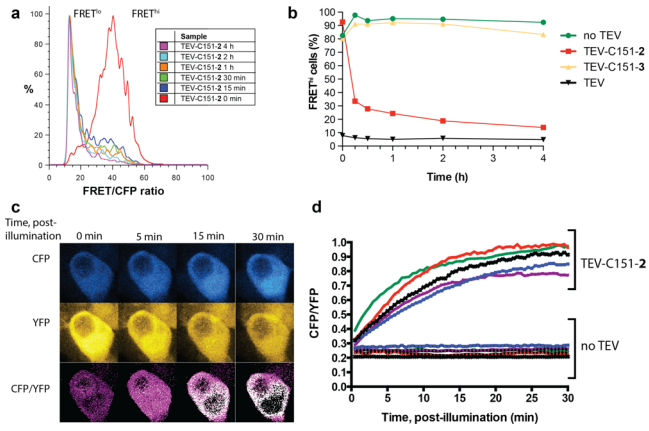

Figure 4. Following TEV protease photoactivation by FRET in mammalian cells. (a) Histograms of FRET/CFP ratio in mCherry positive cells determined by FRET-FACS. (b) Percentage of FRET^{hi} population, for mCherry positive cells, at time points postillumination confirms rapid TEV protease photoactivation. (See SI, Figures S4a−f for detailed FACS analysis). (c) Single-cell analysis of TEV protease photoactivation by live-cell fluorescent imaging. Fluorescent confocal micrographs showing an increase in CFP/YFP fluorescent intensity ratio after illumination in a representative cell expressing FRET sensor and TEV-C151-**2**. (d) Analysis of TEV protease activation in individual cells expressing the FRET sensor and TEV-C151-**2** or cells expressing only the FRET sensor.

experiments demonstrate that cells bearing the CFP-TevS-YFP reporter show a high FRET signal, resulting from energy transfer from CFP to YFP upon excitation of CFP (SI, Figure S4). The FRET signal of the reporter is unchanged upon expression of TEV-C151-**2** or TEV-C151-**3** from a construct containing the *TEV-C151-TAG* gene separated by a self-cleaving T2A sequence[22] from the *mCherry* gene allowing cells containing the construct to be marked with red fluorescence.

In cells bearing TEV-C151-**2**, and illuminated for 1 min, FRET-FACS analysis revealed a shift in the population from high FRET (FRET^{hi}) to low FRET (FRET^{lo}), indicating a decrease in FRET (Figure 4a). This shift occurred within 15 min following illumination, as revealed by the drastic decrease in FRET^{hi} population over time (Figure 4b). In contrast, there was no change in the FRET^{hi} population over time for cells

dx.doi.org/10.1021/ja412191m | J. Am. Chem. Soc. 2014, 136, 2240−2243

containing TEV-C151-**3** and the FRET sensor or cells containing only the FRET sensor. These results confirm that TEV protease can be activated and the FRET sensor in most cells was efficiently cleaved within 15 min.

Single-cell fluorescence microscopy allowed us to follow the activity of TEV protease with greater temporal resolution in live cells (Figure 4c,d). Following photoactivation of TEV protease the CFP/YFP ratio increases within 5 min, and approximately 80% of the FRET sensor in cells is cleaved within 15 min. These results further demonstrate the photoactivation of TEV protease in live cells.

In summary, we have demonstrated the evolution of a pyrrolysyl-tRNA synthetase/$tRNA_{CUA}$ pair for the efficient site-specific incorporation of **2** into proteins in *E. coli* and mammalian cells, the efficient decaging of **2** in proteins expressed in *E. coli* and in mammalian cells and the rapid photoactivation of TEV protease in mammalian cells. By combining the approach reported here with the introduction of TEV sites into proteins of interest it will be possible to create spatially and temporally controlled optically activated protein knockouts. Extending this approach to animals and combining it with emerging genome-editing approaches will allow rapid cell-specific and developmental stage specific photoactivated protein knockouts. We anticipate that this well characterized system for photocontrol of cysteine residues in proteins will form the basis of powerful approaches for rapidly controlling diverse biological processes.

■ ASSOCIATED CONTENT

Ⓢ Supporting Information

Supporting experimental data and procedures. This material is available free of charge via the Internet at http://pubs.acs.org.

■ AUTHOR INFORMATION

Corresponding Author

chin@mrc-lmb.cam.ac.uk

Notes

The authors declare no competing financial interest.

■ ACKNOWLEDGMENTS

Medical Research Council, UK (Grants U105181009 and UD99999908). Trinity College, Cambridge (D.P.N.). EMBO ALTF 1232-2011, Herschel Smith Fund (S.J.E.). Marie Curie Fellowship (C.U.). Jim Wells (UCSF) for T.E.V. and sensor plasmids.

■ REFERENCES

(1) Gautier, A.; Deiters, A.; Chin, J. W. *J. Am. Chem. Soc.* **2011**, *133*, 2124−2127.

(2) Gautier, A.; Nguyen, D. P.; Lusic, H.; An, W.; Deiters, A.; Chin, J. W. *J. Am. Chem. Soc.* **2010**, *132*, 4086−4088.

(3) Kennedy, M. J.; Hughes, R. M.; Peteya, L. A.; Schwartz, J. W.; Ehlers, M. D.; Tucker, C. L. *Nat. Methods* **2010**, *7*, 973−975.

(4) Lemke, E. A.; Summerer, D.; Geierstanger, B. H.; Brittain, S. M.; Schultz, P. G. *Nat. Chem. Biol.* **2007**, *3*, 769−772.

(5) Levskaya, A.; Weiner, O. D.; Lim, W. A.; Voigt, C. A. *Nature* **2009**, *461*, 997−1001.

(6) Wu, Y. I.; Frey, D.; Lungu, O. I.; Jaehrig, A.; Schlichting, I.; Kuhlman, B.; Hahn, K. M. *Nature* **2009**, *461*, 104−108.

(7) Ghosh, M.; Song, X.; Mouneimne, G.; Sidani, M.; Lawrence, D. S.; Condeelis, J. S. *Science* **2004**, *304*, 743−746.

(8) Arbely, E.; Torres-Kolbus, J.; Deiters, A.; Chin, J. W. *J. Am. Chem. Soc.* **2012**, *134*, 11912−11915.

(9) Chen, P. R.; Groff, D.; Guo, J.; Ou, W.; Cellitti, S.; Geierstanger, B. H.; Schultz, P. G. *Angew. Chem., Int. Ed.* **2009**, *48*, 4052−4055.

(10) Deiters, A.; Groff, D.; Ryu, Y.; Xie, J.; Schultz, P. G. *Angew. Chem., Int. Ed.* **2006**, *45*, 2728−2731.

(11) Wu, N.; Deiters, A.; Cropp, T. A.; King, D.; Schultz, P. G *J. Am. Chem. Soc.* **2004**, *126*, 14306−14307.

(12) Davis, L.; Chin, J. W. *Nat. Rev. Mol. Cell Biol.* **2012**, *13*, 168−182.

(13) Li, F.; Zhang, H.; Sun, Y.; Pan, Y.; Zhou, J.; Wang, J. *Angew. Chem., Int. Ed.* **2013**, *52*, 9700−9704.

(14) Bianco, A.; Townsley, F. M.; Greiss, S.; Lang, K.; Chin, J. W. *Nat. Chem. Biol.* **2012**, *8*, 748−750.

(15) Greiss, S.; Chin, J. W. *J. Am. Chem. Soc.* **2011**, *133*, 14196−14199.

(16) Hancock, S. M.; Uprety, R.; Deiters, A.; Chin, J. W. *J. Am. Chem. Soc.* **2010**, *132*, 14819−14824.

(17) Neumann, H.; Peak-Chew, S. Y.; Chin, J. W. *Nat. Chem. Biol.* **2008**, *4*, 232−234.

(18) Mukai, T.; Kobayashi, T.; Hino, N.; Yanagisawa, T.; Sakamoto, K.; Yokoyama, S. *Biochem. Biophys. Res. Commun.* **2008**, *371*, 818−822.

(19) Adams, S. R.; Kao, J. P. Y.; Grynkiewicz, G.; Minta, A.; Tsien, R. Y. *J. Am. Chem. Soc.* **1988**, *110*, 3212−3220.

(20) Nguyen, D. P.; Lusic, H.; Neumann, H.; Kapadnis, P. B.; Deiters, A.; Chin, J. W. *J. Am. Chem. Soc.* **2009**, *131*, 8720−8721.

(21) Gray, D. C.; Mahrus, S.; Wells, J. A. *Cell* **2010**, *142*, 637−646.

(22) Kim, J. H.; Lee, S. R.; Li, L. H.; Park, H. J.; Park, J. H.; Lee, K. Y.; Kim, M. K.; Shin, B. A.; Choi, S. Y. *PLoS one* **2011**, *6*, e18556.